Supporting Information

Synthesis, Acid Properties and Catalysis by Niobium Oxide Nanostructured Materials

M. Luisa Marin, Geniece L. Hallett-Tapley, Stefania Impellizzeri, Chiara Fasciani, Sabrina Simoncelli, Jose Carlos Netto-Ferreira and Juan C. Scaiano

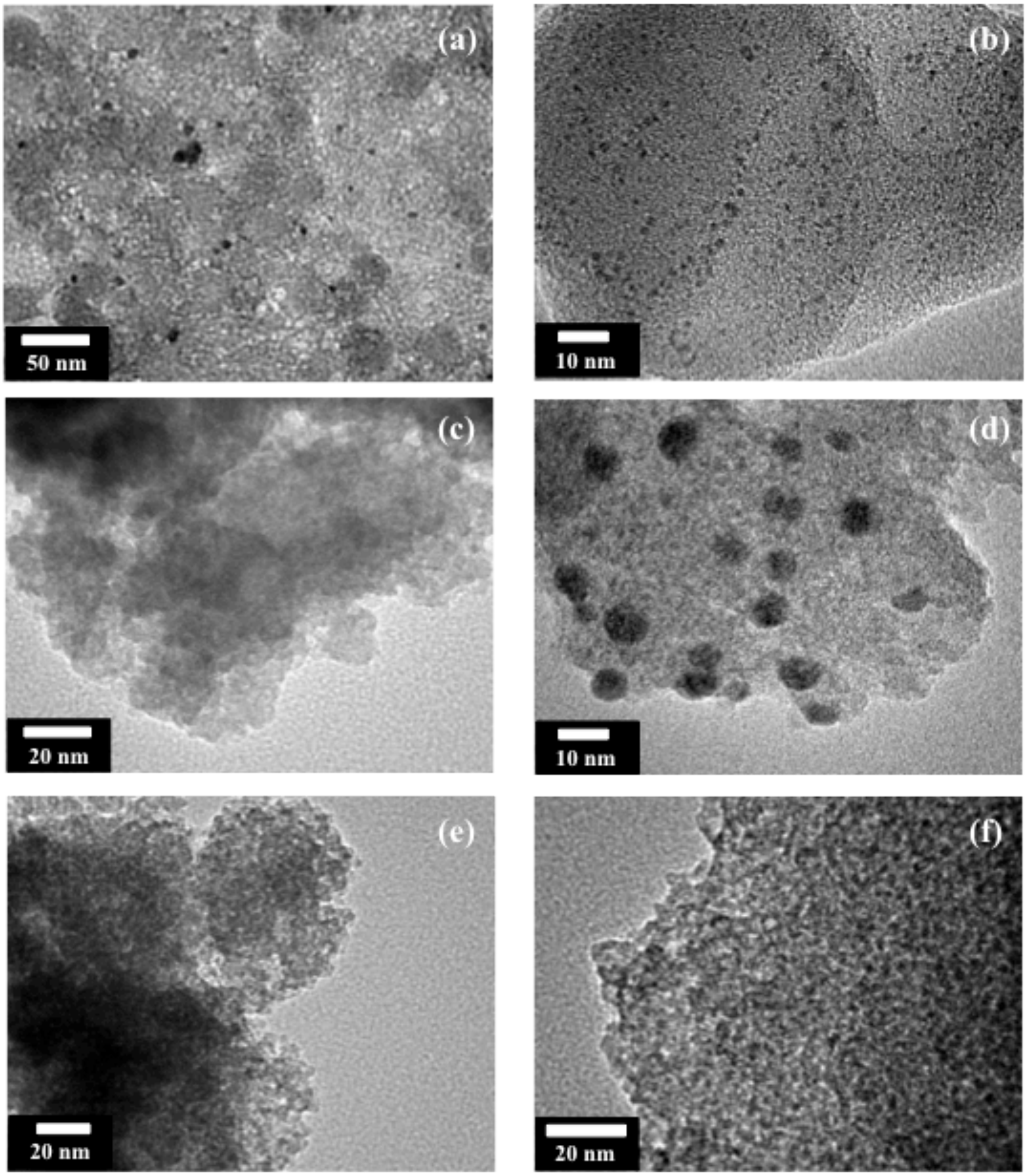

Figure S1. TEM images of (a) comm. $Nb_2O_5{\bullet}nH_2O$, (b) T-I, (c) T-II, (d) T-IIIa, (e) T-IIIb and (f) T-IV.

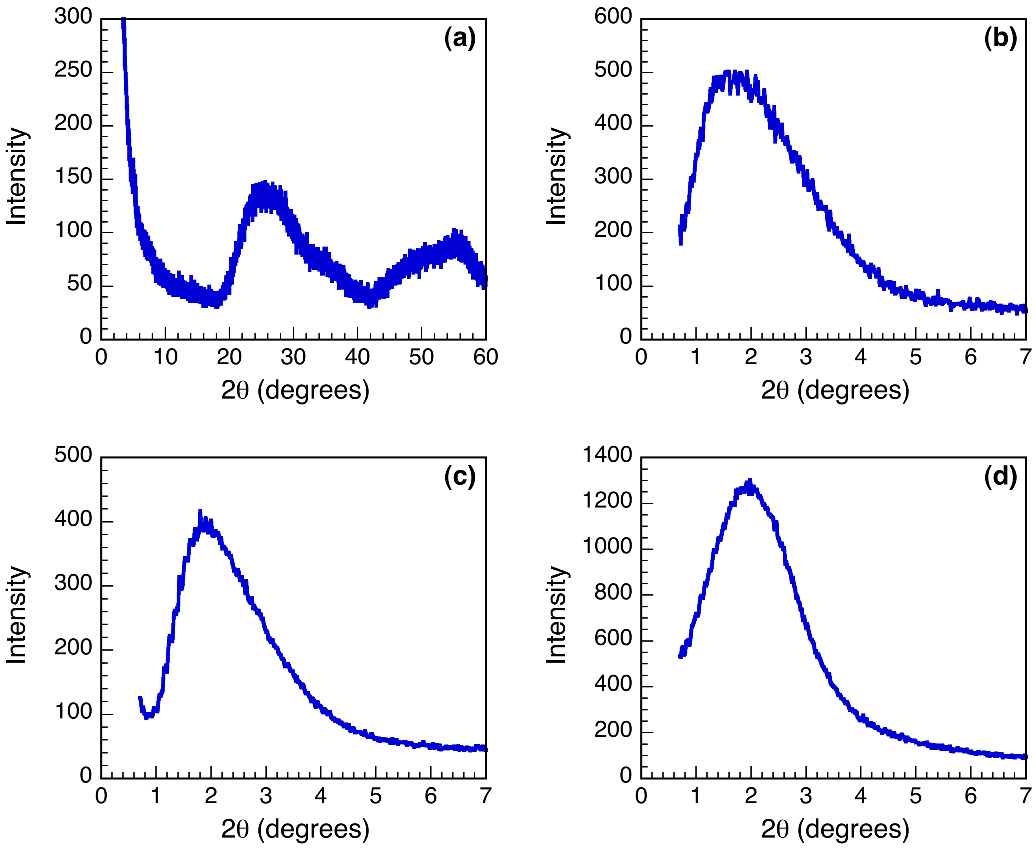

Figure S2. XRD spectra of (a) T-II, (b) T-IIIa, (c) T-IIIb and (d) T-IV.

Table S2. Pore size and surface area data as determined by nitrogen adsorption isotherms.

Sample	BET Surface Area (m^2/g)	Pore Size (Å)
T-IIIa	528	24.4
T-IIIb	295	9.6
T-IV	409	19.6

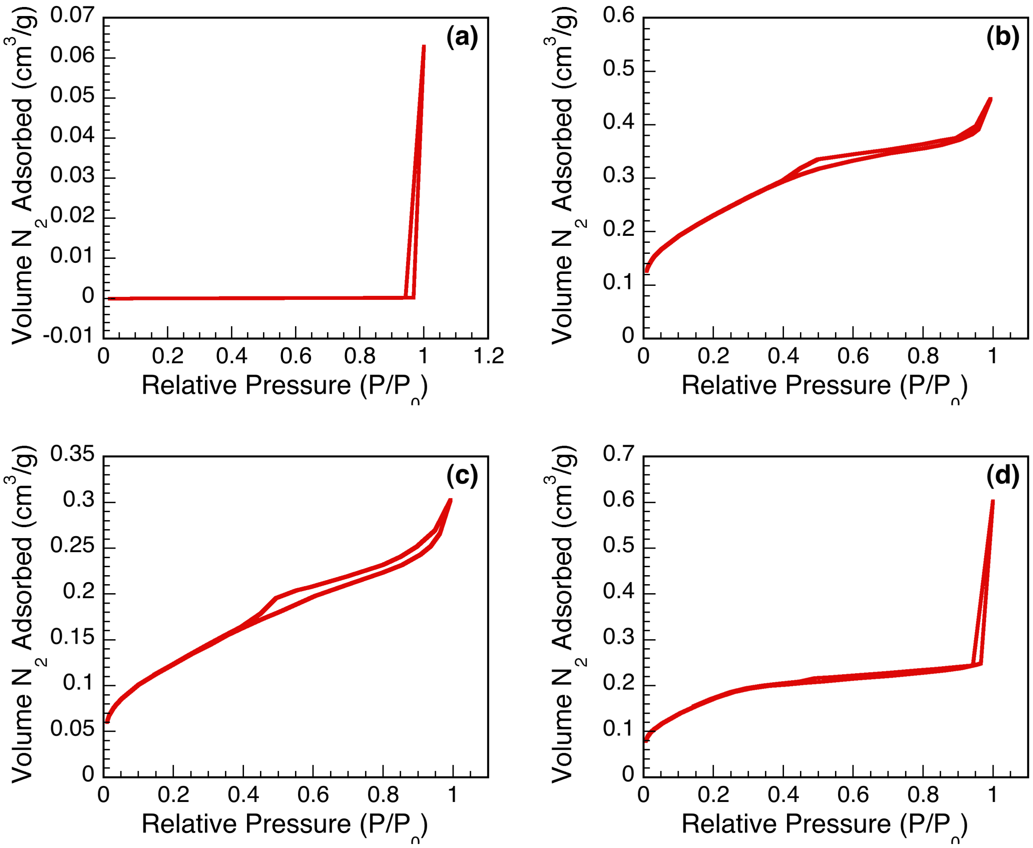

Figure S3. Nitrogen adsorption isotherms of (a) comm. Nb_2O_5, (b) T-IIIa, (c) T-IIIb and (d) T-IV.

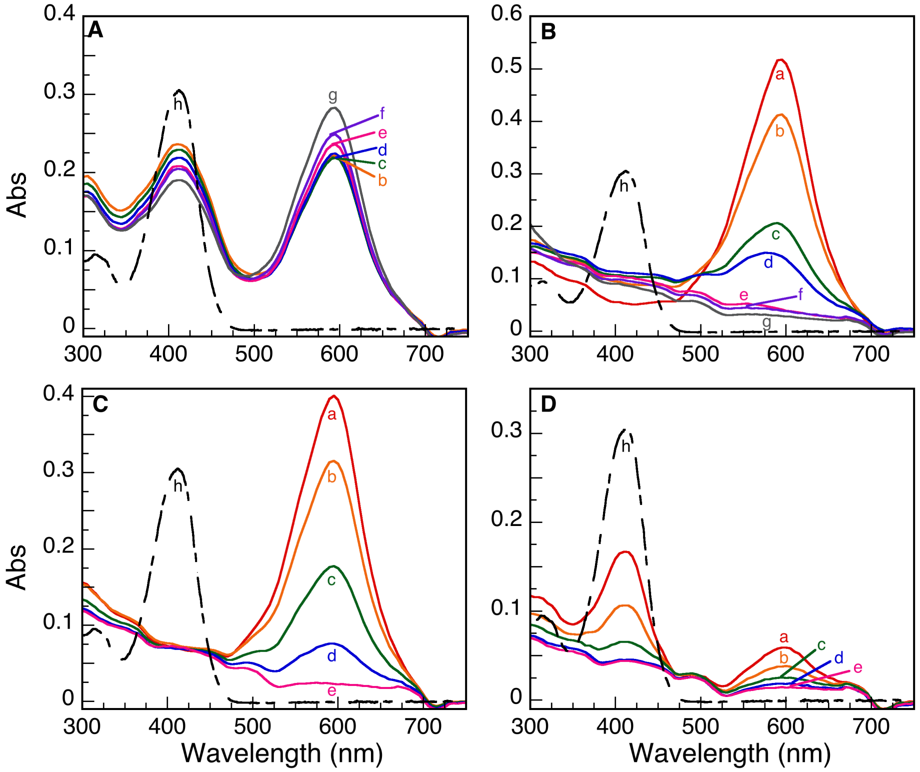

Figure S4. UV-visible spectra monitoring the Brønsted acid ring opening of **1** to **2** using (A) a TFA control (B) T-II, (C) T-IIIb and (D) T-IV as heterogeneous catalysts. The reactions were monitored as a function of time: (a) 0 h, (b) 1 h, (c) 3 h, (d) 5 h, (e) 24 h, (f) 3 d, (g) 5 d and (h) from the initial absorption of **1**.

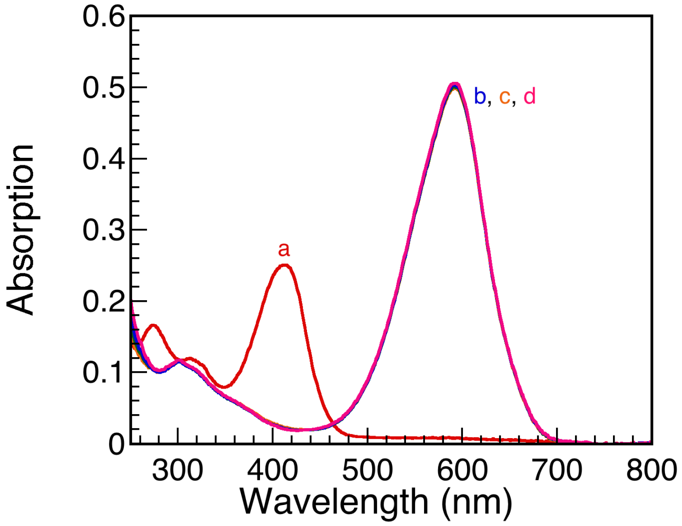

Figure S5. UV-visible spectra monitoring the Brønsted acid ring opening of 7.5 μM **1** under TFA acidic conditions in 14:1 MeCN/H_2O. The reactions were monitored as a function of time: (a) before TFA addition, (b) immediately following TFA addition 0 h, (c) 2 d and (d) 5 d. Note no change in the absorption spectrum as (b), (c) and (d) are all overlapping.

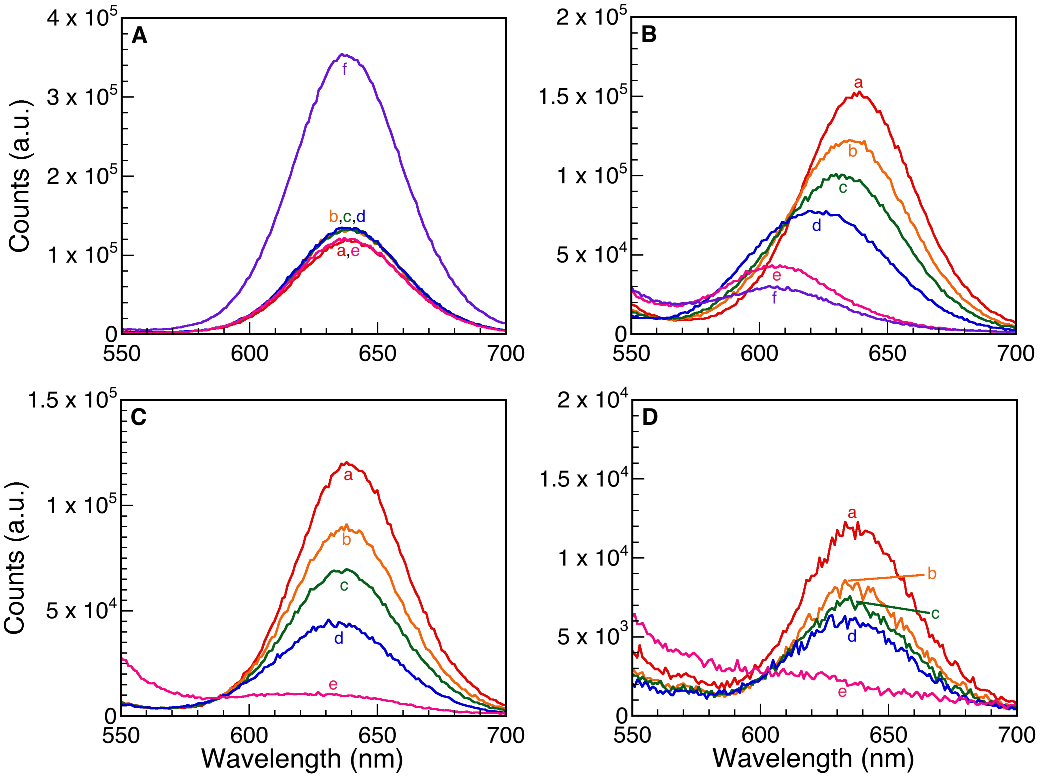

Figure S6. Fluorescence spectra monitoring the Brønsted acid ring opening of **1** to **2** using (A) a TFA control, (B) T-II, (C) T-IIIb and (D) T-IV as heterogeneous catalysts. The reactions were monitored as a function of time: (a) 1 h, (b) 3 h, (c) 4 h, (d) 6 h, (e) 30 h and (f) 4 d.

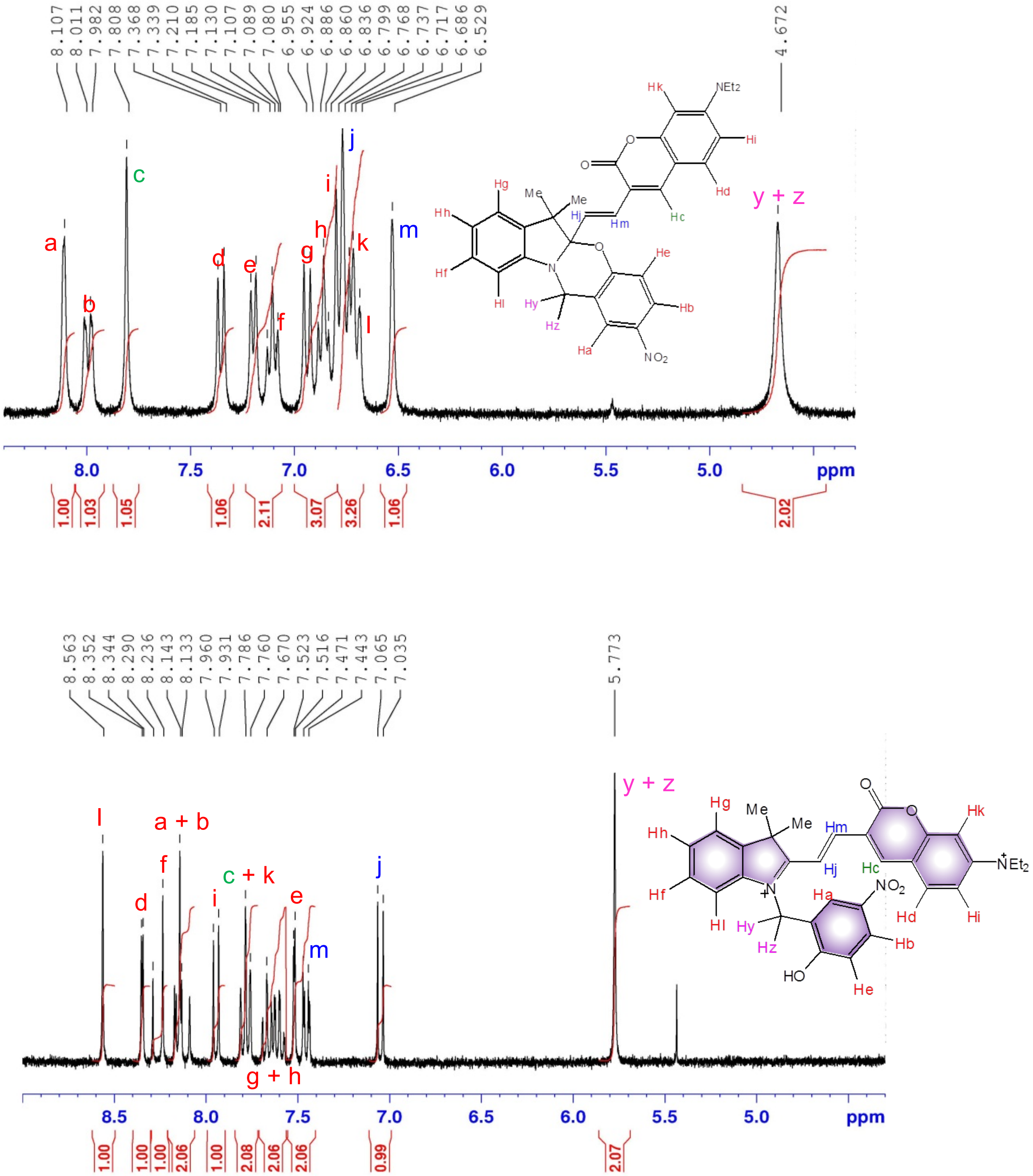

Figure S7. ^{1}H NMR spectra (CD_3CN) and peak attribution of **1** and **2**. The spectrum of **2** was obtained by adding 10 equivalents of TFA to a solution of **1** in CD_3CN. The spectra have been collapsed into the 9-4 ppm region in order to illustrate the peaks most relevant to the discussion. (full ^{1}H NMR enumeration can be found in Ref. 1 of the Supporting Information).

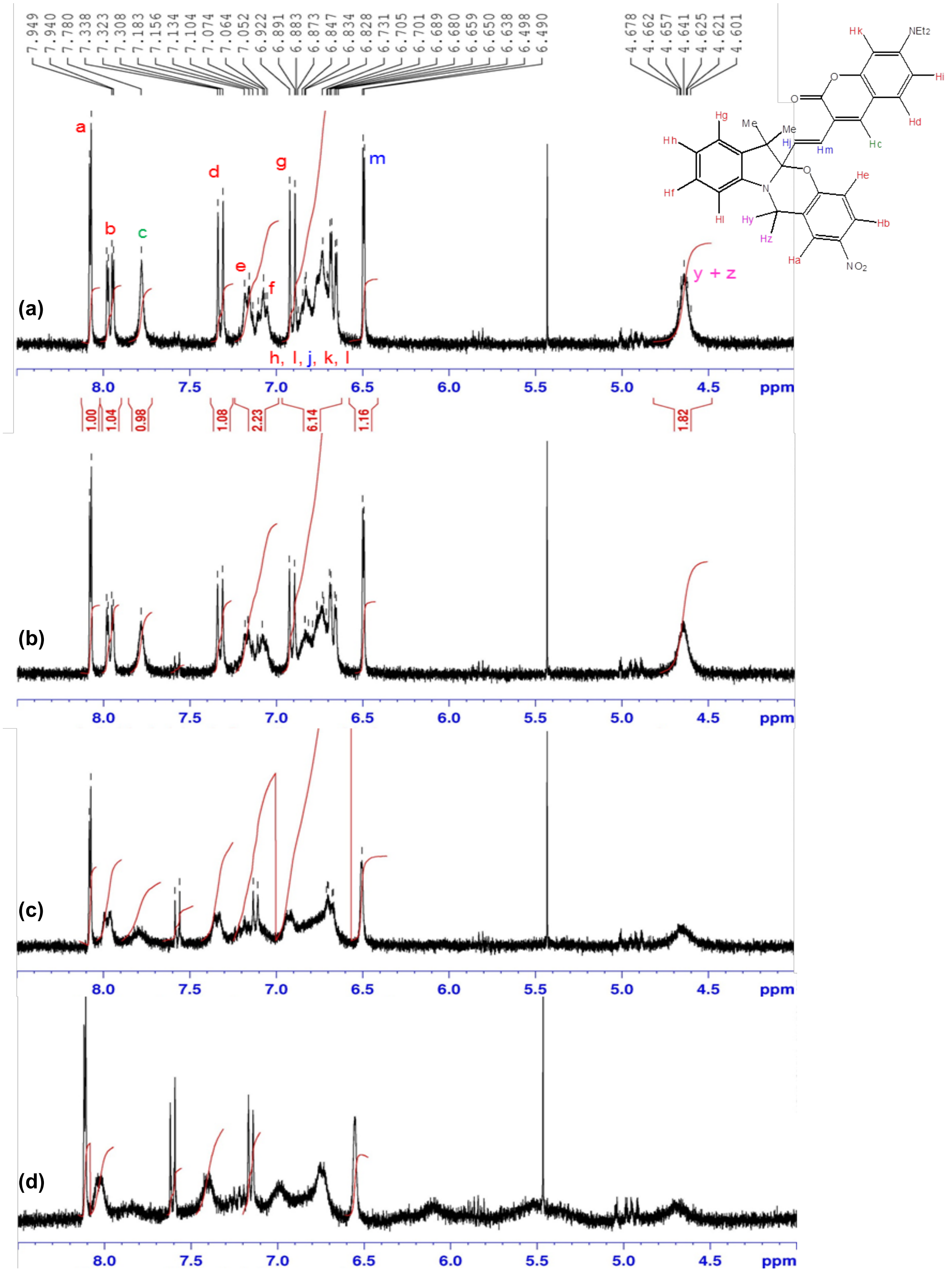

Figure S8. ^{1}H NMR spectra of 1 in CD_3CN (a) immediately, (b) 2 h (c) 24 h and (d) 48 h following the addition of T-IIIa.

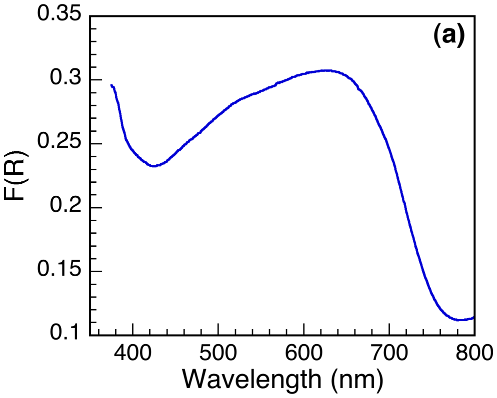

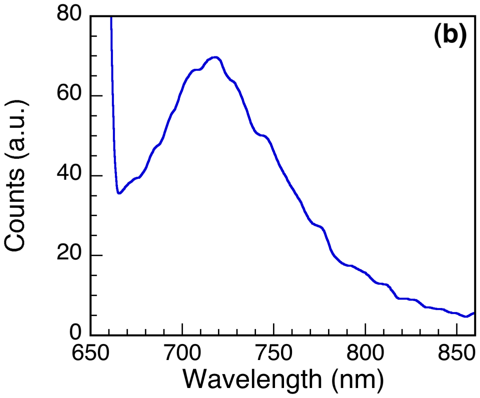

Figure S9. (a) Diffuse reflectance and (b) solid state fluorescence spectra of product **2** adsorbed onto Nb_2O_5•$n$$H_2O$ T-IIIa.

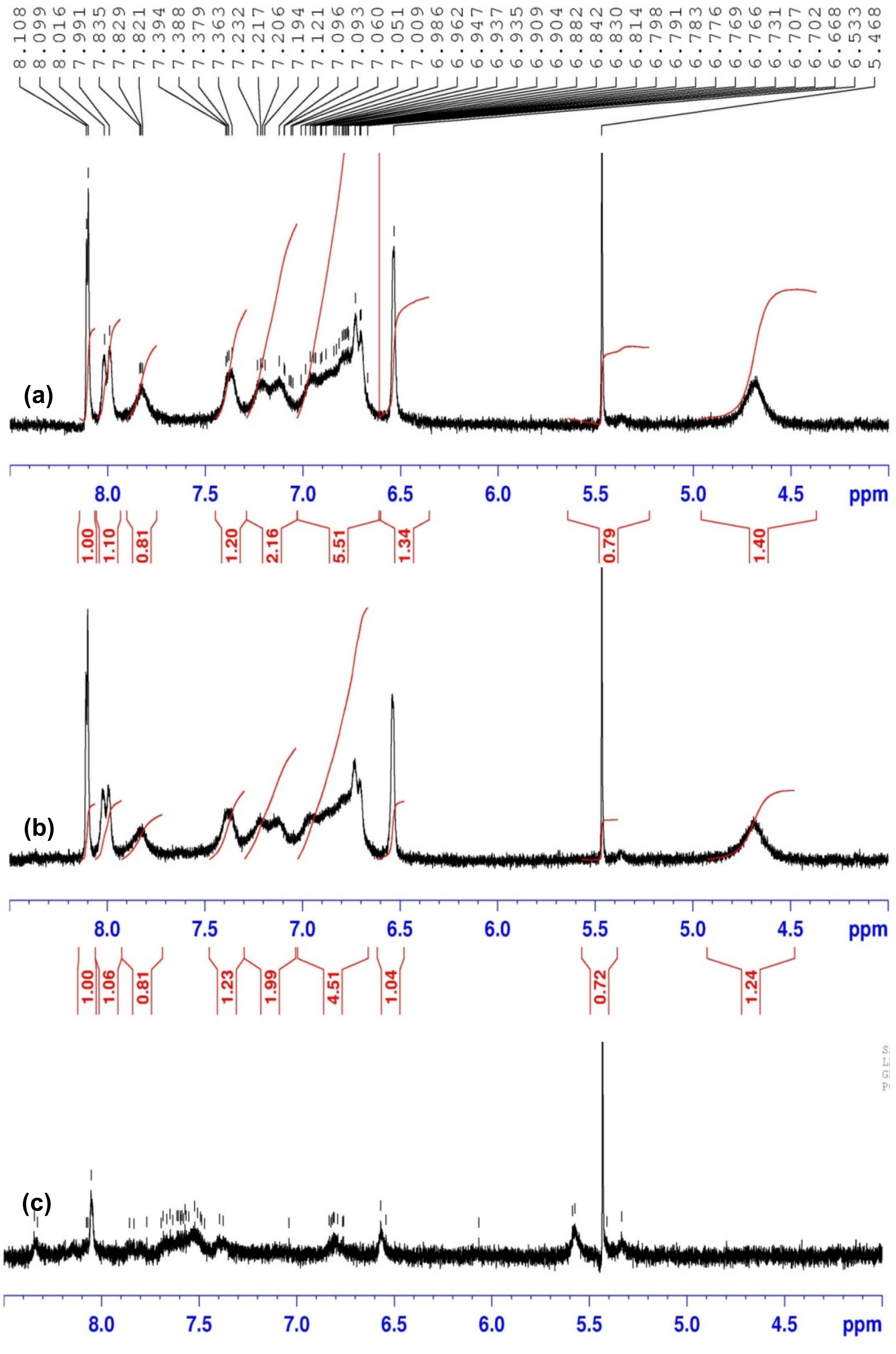

Figure S10. ^{1}H NMR spectra of **1** in CD_3CN (a) immediately, (b) 2 h and (c) 96 h after the addition of Nb_2O_5•$n$$H_2O$ T-I.

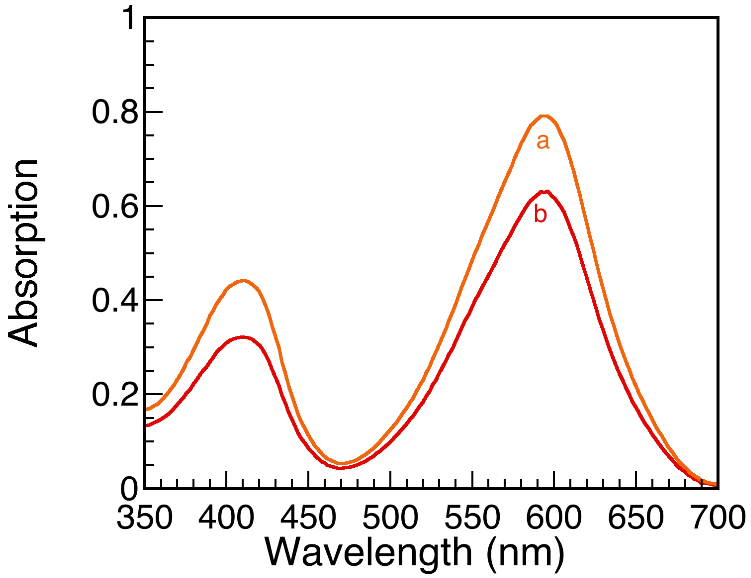

Figure S11. UV-visible spectra monitoring the reusability of catalyst **T-I** in the Brønsted acid ring opening of 150 μM **1** to **2** (40 mg of **T-I** in 10 mL of MeCN) following 1 day of reaction: (a) Trial 1 and (b) Trial 2.

Note: Catalyst recovery and use was carried out as follows-

Following one day of reaction, the catalyst was recovered by centrifugation at 3500 rpm for 10 minutes in a 15 mL Falcon tube. The supernatent was decanted and saved for analysis, while the catalyst was washed 5 times with 5 mL of MeCN and then left to dry overnight in the fumehood. The following day, the catalyst was placed under vacuum for 3 hours to remove any residual MeCN. The catalyst was then weighed and the reaction scaled down accordingly to obtain the same concentrations of catalyst to substrate **1** as was stated in the initial reaction.

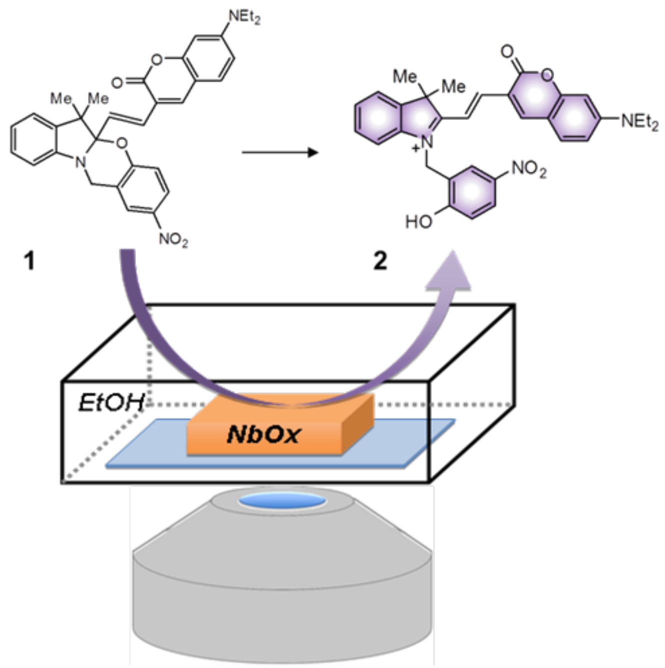

Figure S12. Schematic representation of the experimental set up for single-molecule fluorescence observation under TIRF illumination (λ_{ex} = 633 nm, 40 W/cm^2) for the Brønsted acid-catalyzed isomerization of **1** (non-fluorescent) to product **2** (fluorescent) over a single $Nb_2O_5 \bullet nH_2O$ T-I particle.

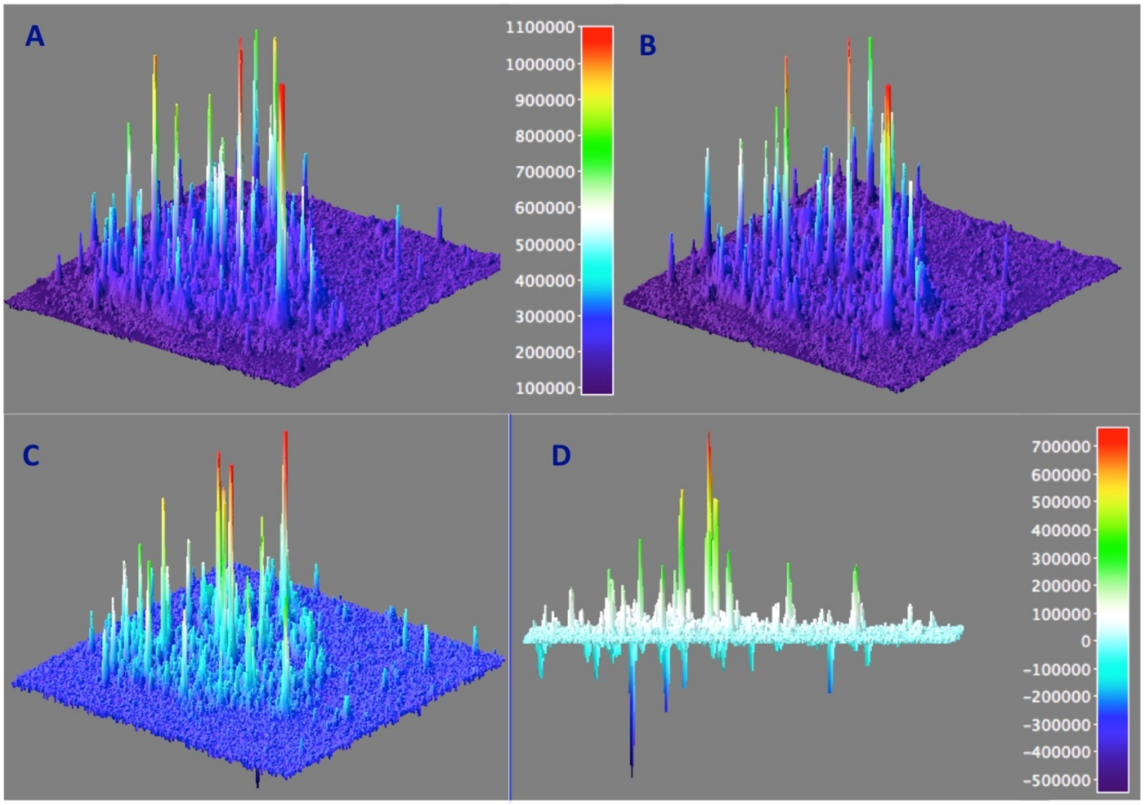

Figure S13. Protonation activity as shown by the conversion of **1** to **2** and detection of the fluorescence from **2**. Surface maps A and B depict the accumulated signals for the first 25 seconds and the subsequent 25 seconds of reaction, respectively. Map C presents the differences of A minus B expanded by an approximate factor of 3. Panel D shows an alternative view of panel C, illustrating both positive and negative peaks (see colour coded scale). Note that this figure is related to the one represented in Figure 7 in the manuscript.

References

1) E. Deniz, S. Sortino, F. M. Raymo, *J. Phys. Chem. Lett.*, **2010**, *1*, 3506-3509.